Modeling of collisionless and kinetic effects in thruster plasmas

IEPC-2005-096

Presented at the 29th International Electric Propulsion Conference, Princeton University, October 31 – November 4, 2005

Igor D. Kaganovich*
Plasma Physics Laboratory, Princeton University, Princeton, NJ, 08543, USA

Abstract: Plasmas used in electric propulsion often operate at low-pressures, where particle mean free path is large compared with thruster dimensions. As a result, the collisionless effects become important and kinetic treatment has to be performed for plasma modeling. For the sake of simplicity, modelers frequently use fluid approach outside of its validity range. On a number of examples it is shown that the fluid approach can lead to quantitatively and qualitatively incorrect results. In fluid approach, the electron energy distribution function (EEDF) is assumed to be a Maxwellian. At low pressures it is no longer the case; and EEDF can be far from a Maxwellian. Electrons tend to stratify into different groups depending on their origin and confinement, i.e., weather they are trapped or not by the plasma potential. These different groups of electrons have to be treated separately, as they have completely different properties and, by no means, can be lumped together into one Maxwellian EEDF, as implicitly assumed by the fluid approach. These facts are well-known in gas discharge community but have not fully propagated into the propulsion community so far. The concept is demonstrated on an example of calculation of particle and heat losses from bounded plasma in presence of strong secondary electron emission as pertains, but not limited to a Hall thruster. Another example is plasma jet's radial expansion in presence of strong axial magnetic field. The "conventional wisdom" approach predicts a conical shape for the plasma jet. This stems from the assumption that electrons and ions diffuse together across the magnetic field lines with an effective ambipolar diffusion coefficient taking from one-dimensional theory. However, such "conventional wisdom" approach fails in two-dimensional geometry, because electrons and ions trajectories are very different in 2D. Electrons can flow fast along the magnetic field lines and simultaneously diffuse radially far from jet injection point and then come back along another magnetic field line. As a result, ions flow freely to the radial position where electrons are available due to such complex loop-like electron trajectories. These short-circuiting flows result in a cylindrical shape of the jet in contrast to conical. A practical application of this result can be analysis of differences between testing, laboratory environment and real space environment.

Nomenclature

T_e = electron tempreture
ϕ_{sh} = plasma potential at sheath plasma sheath boundary
ϕ_w = wall potential
$\Delta\phi_{sh}$ = potential drop in the sheath

* Research Physicist, Theory Department, ikaganov@pppl.gov.

ε = total electron energy: sum of kinetic and potential energies
m = electron mass
M = ion mass
v_x = x component of the electron velocity
$\Gamma_w(\varepsilon)$ = the electron flux to the wall with total energy ε
ν = elastic collision frequency
n = electron density

I. Introduction

Recently, the low-pressure high-density plasmas have attracted considerable interest for propulsion and material processing applications[1,2]. Typically, the operating gas pressures in such plasmas range from 10^{-5} Torr to 10^{-2} Torr. Correspondingly, the electron mean free path can be larger or comparable to the plasma dimensions (typically several tens of centimeters). As a result a number of collisionless and kinetic effects become important for correct plasma description and are frequently misinterpreted by application of "conventional wisdom" approaches based on fluid or one-dimensional results. In the following three such examples are given. First, the importance of non-Maxwellian electron energy distribution is demonstrated for low-pressure plasmas. Second, the kinetic concept is demonstrated on an example of calculation of particle and heat losses from a bounded plasma in presence of strong secondary electron emission as pertains, but not limited to a Hall thruster. It is shown that conventional concept of space charge limited sheath is inadequate due to oversimplified assumption of the Maxwellian electron energy distribution function. It is shown that the kinetic approach gives completely different result and explain experimental data, whereas the fluid approach fails to do so. The last example describes plasma jet's radial expansion in presence of strong axial magnetic field. The "conventional wisdom" approach foresees a conical shape for the plasma jet, whereas detailed analysis calculates a cylindrical shape.

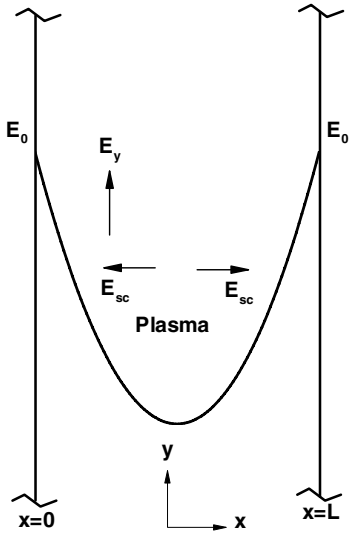

Figure 1. Schematic of a one-dimensional plasma slab of length L powered by a symmetric coupled source. The RF current source (not shown) results in an RF field in the transverse direction, E_y. The value of the field at the edges, E_0, is determined by the desired power deposition in the plasma. A space charge field E_{sc} develops in the x-direction to confine electrons.

II. Importance of self-consistent calculation of non-Maxwellian electron energy distribution function

A. Examples of non-Maxwellian electron energy distribution function in discharges

Under low-pressure conditions, the electron energy distribution function (EEDF) is far from a Maxwellian. The EEDF can be enriched by slow electrons[3], as well as the EEDF can have pronounced high energy tail[4] or abrupt cut-off at energies corresponding to plasma potential[5]. The high-energy electrons determine the dissociation and ionization rates. The slow energy electrons are responsible for the formation of the ambipolar potential in the plasma bulk. In low-pressure plasmas the EEDF, plasma density and electric field in plasma are all nonlinear coupled. Such

nonlinear coupling may lead to novel kinetic phenomena, for example, it was demonstrated in Ref.6 that the formation of two-temperature EEDF could be accompanied with an explosive increase in the bulk plasma density.

We have developed variety of tools for kinetic analysis of low-temperature plasmas, including particle-in-cell codes, fast modeling codes and analytical theories[1-6].

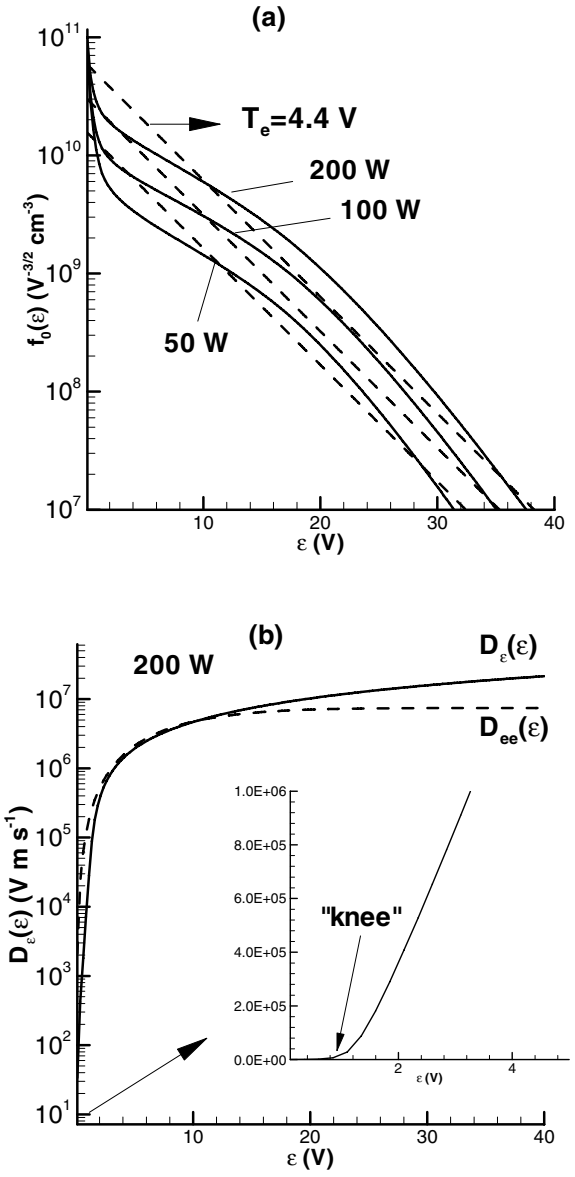

Figure 3. (a) Self-consistently predicted non-Maxwellian (solid lines) and Maxwellian (dashed lines) electron energy distribution function (EEDF) as a function of total energy for 1 mTorr. (b) Energy diffusion coefficient $D_\varepsilon(\varepsilon)$ (solid line) and energy diffusivity (see text) related to e-e collisions (dashed line) as a function of total energy for 1 mTorr. Inset shows an expanded scale for $D_\varepsilon(\varepsilon)$.

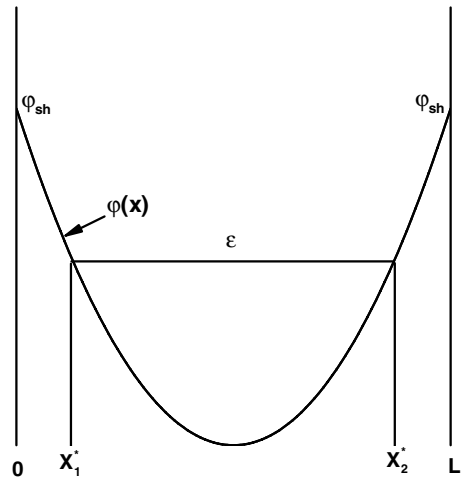

Figure 2. Schematic of electron potential energy profile $\varphi(x)$ in the plasma slab, due to the electrostatic field. An electron with total (x-kinetic plus potential) energy ε will reflect back at points x_1^* and x_2^* (turning points).

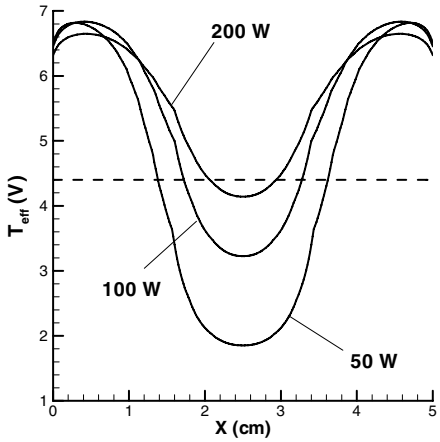

Figure 4. Effective temperature profiles for a non-Maxwellian EEDF (solid lines) and a Maxwellian EEDF (dashed lines) for 1 mTorr.

Typical results are shown in Figs. 3-5 on example of an inductively rf coupled plasma of a pressure of 1 mTorr, discharge frequency of 13.56 MHz and discharge length 5 cm[7]. Similar results have been received for other low-pressure plasmas including electron cyclotron resonance, capacitively coupled and

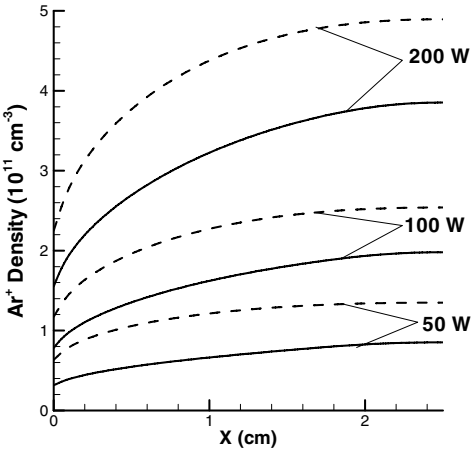

Figure 5. Variation of positive ion density for 1 mTorr. Results using non-Maxwellian EEDF (solid lines) are compared with results using Maxwellian EEDF (dashed lines), under otherwise identical conditions.

direct current discharges. Figures 1 and 2 show the schematics of heating rf electric field and ambipolar electric field which confines electrons in the plasma center due to ambipolarity constrain. Under these conditions the electron-electron collision mean free path and inelastic collision mean free path are large compared to the plasma dimension. Due to large value of mean free path, electrons have the total energy $\varepsilon = mv^2/2 - e\phi$ constant. Electrons with small ε are confined in the plasma center in the region of small electric field, whereas electrons with large ε approach plasma periphery where the electric field is large. As a result, the EEDF is strongly non-Maxwellian, as shown in Fig.3. Figure 3 shows the EEDF as a function of total energy for non-Maxwellian (solid lines) and Maxwellian (dashed lines) cases. The non-Maxwellian EEDF has a higher fraction of electrons just beyond the ionization threshold, predicting a higher ionization rate.

Figure 4 shows the screening temperature profiles given for the Maxwellian and non-Maxwellian EEDFs. The screening temperature is defined to give value of the ambipolar electric field $E = -T_e(x)\nabla n/n$. For the Maxwellian EEDF, the electron temperature is uniform and independent of power while for the non-Maxwellian case, significant differences are observed with power. The large difference between the temperatures at the edge and the center may be explained by examining Fig. 3 (solid lines). The EEDF shows that electrons with total energies less than 1 V are not effectively heated (the energy diffusion coefficient D_ε is small). Electrons with such low energies are trapped near the discharge center (where the heating field is weak) as they cannot overcome the electrostatic potential barrier. Hence, the effective temperature at the center is low. In contrast, electrons with relatively high energies can overcome the potential barrier and reach the edge where the field is strong, and the effective temperature at the periphery (and larger total energies) is high. Note that even for the highest plasma density in Fig. 3, the electron-electron mean free path is about 10 m for 1 eV electrons, much higher than the interelectrode gap. Therefore, the electron-electron and collisionless energy diffusion coefficients are comparable at very low energy, 1 eV, see Fig. 3. As a result, low energy electrons form a Maxwellian distribution with very low temperature, 1 eV. Note that the part of the EEDF corresponding to such cold electrons is difficult to measure experimentally. The effective temperature profile becomes less non-uniform as power is increased, because of higher electron density resulting in more "thermalization" of the EEDF by e-e collisions. The discrepancy between the averaged temperature and the effective temperature near the edge induces a difference in the effective electron mean free path, which leads to considerably different profiles of power deposition.

Plasma density profiles calculated using the non-Maxwellian EEDF (solid lines) are compared with profiles (dashed lines) obtained using the Maxwellian EEDF approximation swon in Fig.5. It is evident, that the calculated plasma parameters can drastically depend on the shape of EEDF due to difference in ionization profile and ambipolar electric field. This suggests that the realistic plasma simulations must necessarily include the self-consistent treatment of non-equilibrium EEDF.

B. Electron energy distribution in the loss cone

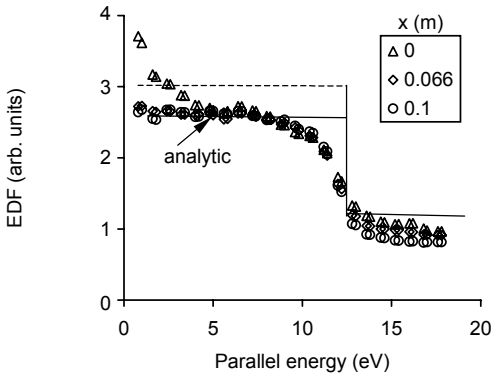

Figure 6. EEDF at given total energy 1.5 of wall potential as a function of the parallel energy at various coordinates, solid lines correspond to the theoretical estimate and dashed lines to the estimate with the total cross-section replaced with the averaged cross-section of scattering outside the loss cone at p=1mTorr. Wall potential is 12.4eV.

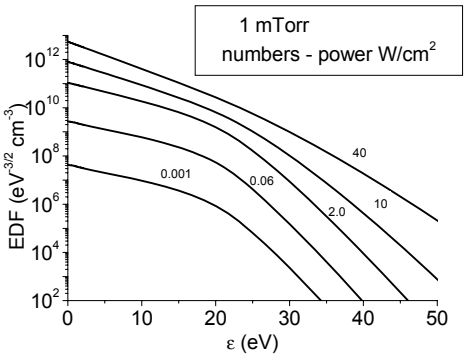

Figure 8. The EDFs as a function of the total energy calculated from the self-consistent calculations. The ECR resonance is in the discharge center.

The potential drop in the sheath determines the particle and heat fluxes from plasma to the bounding walls. In "common wisdom" approach the potential drop in the sheath is given by $\Delta\phi_{sh} = -T_e / e \ln(M / m2\pi)$, where M, m are the ion mass and electron mass, respectively. The derivation assumes Maxwell-Boltzmann distribution of electrons. However, Boltzmann distribution of electrons requires that electrons are trapped by the field, whereas we calculate the flux of electrons leaving the plasma, i.e., untrapped electrons. Thus, the conventional expression for sheath potential drop is incorrect[8]. The electrons which have energy sufficient to overcome the sheath potential, quickly escape the plasma, thus, this part of EEDF is strongly depleted and often termed as loss cone in phase space. The analytical solution for the EEDF in the loss cone was derived in Ref.9. The electron distribution function in the loss cone is filled due elastic scattering which transfer electrons from outside of loss cone to loss cone, and emptied by free flight to the wall with rate determined by the transit time. The total flux of electrons from loss cone $\Gamma_w(\varepsilon)$ with a given energy ε is given by [9]

$$\Gamma_w(\varepsilon) = \int_{v_{x\min}}^{v} \frac{dv_x}{v} v_x f_0 \left[1 - \exp\left(-\int_{-L/2}^{L/2} \nu dx / v_x\right)\right] \quad (1)$$

where ν is the elastic collision frequency, $v_{x,\min}$ is minimum velocity of electrons capable to overcome sheath potential and escape to the wall, integration is done over all velocity directions contributing into the flux. The average escape frequency is than given by ratio of this flux to the total density of electrons $\nu_{escape} \equiv \Gamma_w(\varepsilon) / f_0 L$. If the electron mean free path is small compared with gap, then the exponent on the right hand side of Eq.1 is small and the conventional estimate for the flux is correct. In the opposite case of large mean free path, the exponent on the right hand side of Eq.1 is close to unity, and

$$\nu_{escape}(\varepsilon) = \int_{v_{x\min}}^{v} \frac{dv_x}{vL} v_x \int_{-L/2}^{L/2} \frac{\nu dx}{v_x} \sim \nu \frac{\Delta_{ec}\Omega}{4\pi} \quad (2)$$

is proportional to the frequency of elastic scattering from outside of loss cone to the loss cone

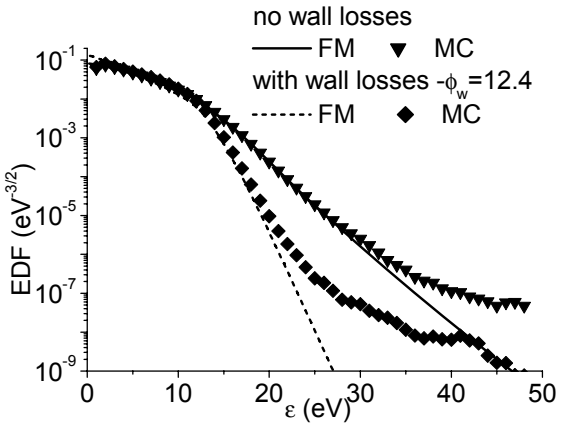

Figure 7. The EDFs calculated from the averaged kinetic equation (lines) and by the MC method (symbols) as a function of the total energy with account for wall losses (dashed lines) and without account for wall losses (solid lines), electric field at electron cyclotron resonance 0.7 V/cm, p=1mTorr, wall potential 14.2eV.

of geometric angle $\Delta_{ec}\Omega$. Figure 6 depicts EEDF outside and inside of the loss cone calculated by a Monte Carlo (MC) code. One can see, that the theoretical prediction for uniform EEDF outside the loss cone is reasonable within 20%.

Figure 7 depicts EEDFs calculated with and without taking into account wall losses making use of the analytical formulation utilizing averaged kinetic equation and Monte Carlo methods for a given wall potential. Both results agree for electron energies up to $\varepsilon < 2e \mid \phi_w \mid$. For higher energies the values of the EEDF calculated by MC code are much higher than theoretical predictions. The reasons are not clear. Possibly the concept of diffusion in energy fails, since electrons of these energies are not trapped and leave the discharge with a frequency about the bounce frequency. It implies that there are not many bounces in the resonance region anymore and averaging over many interactions with resonance is not adequate.

Figure 8 shows EEDF when wall potential is calculated from the ambipolarity condition. Due to fast wall losses the effective temperature at the EEDF tail $\varepsilon > e \mid \phi_w \mid$, is 2.2eV instead of 6.6eV in the plasma bulk. Potential drop in the sheath is 17eV, which is much smaller than $\Delta\phi_{sh} = -T_e / e \ln(M / m2\pi)$ =4.7Te=31eV. Here, the argon mass was assumed.

III. Effects of non-Maxwellian EEDF on particle and heat losses from a plasma in presence of secondary electron emission

The sheath near wall is strongly affected by the secondary electron emission from the wall. If the secondary electron emission current is larger than the primary electron current from the plasma, i.e., the effective secondary electron emission coefficient becomes large than unity, ambipolarity condition of zero total current can not be satisfied by a monotonic sheath. In this limit, the sheath potential drop becomes very small and electron particle and heat fluxes from the plasma turn out to be very large. In case of bounded plasma the fluxes of secondary electrons can greatly affect plasma properties. The fact well-known for gas discharges since 1950s[10]. In case of bounded plasmas there are two counterstreaming electron beam coming from opposite walls. Presence of two beams greatly effects sheath properties compared with the case of semi-infinite plasma. The secondary electron emission (SEE) of the beams have completely different properties than the bulk plasma, thus, they have to be treated separately. Consequently, we introduce two partial secondary electron emission coefficients of the plasma bulk, γ_p, and of the beam, γ_b. The plasma electron flux F_p at left wall generates SEE flux $\gamma_p F_p$, which propagates with certain probability to the right wall, resulting in an additional flux of secondaries at the right wall $\alpha\gamma_p F_p$. Here, we introduced the penetration coefficient $\alpha < 1$, the SEE beam losses are due to scattering and deceleration by collective effects and collisions. The SEE flux $\alpha\gamma_p F_p$ produces extra SEE flux $\alpha\gamma_b\gamma_p F_p$, which propagates to the left and generate additional SEE flux, and so forth. The ratio between the resulting total SEE fluxes F_b and the plasma bulk flux F_p is given by the balance between them. The total flux hitting the left wall is $\alpha F_b + F_p$. It generates SEE flux F_b, i.e.,

$$F_b = \gamma_b \alpha F_b + \gamma_p F_p , \tag{3}$$

which gives

$$F_b = \frac{\gamma_p}{1 - \gamma_b \alpha} F_p . \tag{4}$$

Note that if $\alpha\gamma_b > 1$ the stationary solution is impossible, as the SEE flux increases after each pass through the plasma even without contribution from the plasma electrons. The other important consequence of Eq.(4) is that if $\alpha\gamma_b \to 1$, the SEE flux is much larger than the plasma flux and can dominate the electron conductivity. This fact was observed in particle-in-cell simulations in Ref.11. The electric current at a wall is sum of contributions from ion flux F_i, plasma bulk and SEE fluxes

$$j / e = F_i - (1 - \gamma_p) F_p - (1 - \gamma_b) \alpha F_b . \tag{5}$$

Substituting the SEE flux from Eq.(4) into Eq.(5) gives

$$j/e = F_i - \left[1 - \frac{(1-\alpha)\gamma_p}{1-\alpha\gamma_b}\right] F_p . \qquad (6)$$

The plasma potential on dielectric wall is given by $j = 0$. If $\alpha \to 1$, the SEE contribution into the total current from the left and right walls mutually compensate each other and presence of beams do not change the sheath properties. Importantly, in this case, the partial plasma SEE coefficient can be large, $\gamma_p >> 1$, without the space charge saturation. This conclusion can explain the experimental results for the Hall thruster[12]. The space charge saturation occurs when contributions into j from all electron currents tends to zero, i.e., $1-(1-\alpha)\gamma_p/(1-\alpha\gamma_b) \to 0$ or $\alpha\gamma_b + (1-\alpha)\gamma_p \to 1$. Note that it is important to introduce different partial SEE coefficients γ_p and γ_b. The further details of analytical calculation of EEDF and SEE beams can be found in Ref. 13. The results of analytical model of Ref.13 are shown in Fig. 9 for $\alpha = 0.9$. As the electron temperature grows both γ_p and γ_b increases. The plasma potential decreases and the electron flux to wall increases when $\alpha\gamma_b + (1-\alpha)\gamma_p \to 1$, and $\gamma_p \approx 2.2$. The EEDF in particle-in-cell simulation of Ref.11 shows that cut-off of EEDF (the loss cone) occurs at wall potential as described above. The simulations also reveal that in thruster plasmas the EVDF is anisotropic and far from a Maxwellian. The average energy of electron motion in the directions parallel to the walls is several times larger than the energy perpendicular to the walls. The strong heating occurs in the direction of the electric field and in plane perpendicular to the applied magnetic field due to scattering in fluctuations of the turbulent electro-magnetic field. The EVDF cannot be isotropized by collisions with neutrals because for the chosen parameters, the effective frequency of turbulent collisions is much larger than the elastic collision frequency. Taking into account the non-Maxwellian EEDF is also very important for analysis of the two-stream instability of SEE beam, which determines the penetration coefficient α.

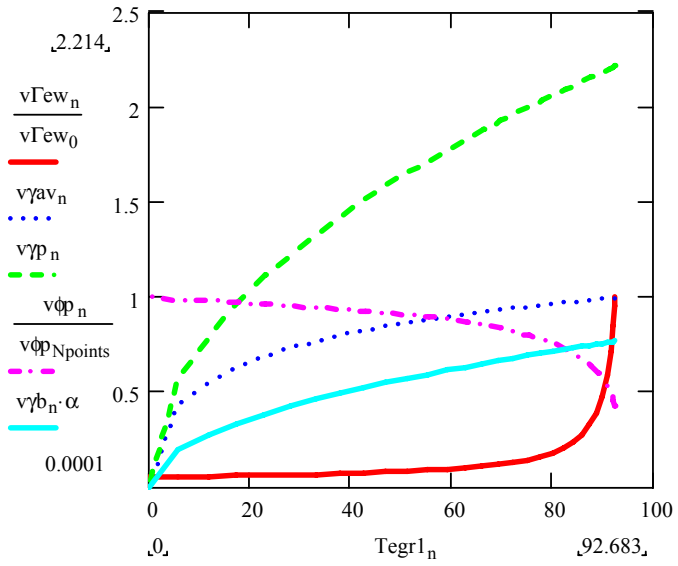

Figure 9. The normalized electron flux Γ_{pn} (red), average SEE coefficient $<\gamma>$ (blue), plasma SEE coefficient γ_p, normalized sheath potential (magenta) and beam SEE coefficient times the penetration factor $\alpha\gamma_b$ as functions of the electron temperature in bulk plasma.

In summary of this section, the kinetic treatment of particle and heat losses from a plasma in presence of secondary electron emission gives drastically different results than the fluid approach. The further details of analytical calculation of EEDF and SEE beams can be found in Ref. 13.

IV. CONTROLLING A MAGNETIZED PLASMA JET'S EXPANSION FOR ELECTRIC-PROPULSION APPLICATIONS

For plasma propulsion it is important to make sure that laboratory testing is adequate to space testing and to control the plasma jet's radial expansion. For this detailed analysis of jet radial expansion is necessary. Applied magnetic fields and the geometry of boundaries surrounding the jet are two methods to control expansion. Plasma jets are predominantly quasineutral, hence, electrons and ions tend to move in applied magnetic fields and induced

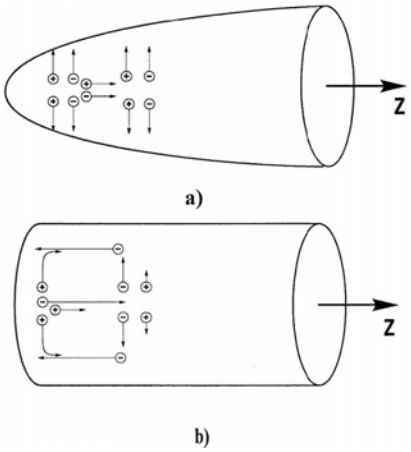

Figure 10. The scheme of non-ambipolar diffusion accompanied by short-circuiting currents. Arrows show the electron and ion motion. The arrow length represents the value of particle fluxes. (a) Hypothetical ambipolar expansion. (b) Real non-ambipolar fluxes.

plasma electric and magnetic fields in such ways that the plasma stays quasineutral[14], except in small regions known as double layers. Due to the big difference in mass, electrons and ions trajectories are very different. That makes the problem of jet expansion rather complex and interesting. In many plasma thrusters, electrons are strongly magnetized and can not detach easily from the magnetic lines. This electron "stiffness" can produce plasma polarization, and, in principle, may hinder ions from detaching from magnetic field lines. Figure 10 shows the effect of polarization in modeling jet motion along and expansion across a uniform magnetic field [2] when electron-ion collisions are included. Ions expand radially across the magnetic field to locations where electrons can be supplied to neutralize the ion density. At radii larger than 2 in Figure 11, ion radial expansion is stopped by an electric field generated by a small charge separation. The quasineutrality condition holds due to the so-called short-circuiting effect: electron flow along magnetic field lines from larger radii back to the jet entry point.

To illustrate an important effect of nonlocal currents, we consider the case of a finite diameter plasma stream entering a region with an axially uniform magnetic field. One might suppose that the radial expansion of the stream is set by a local ambipolar condition, that is, collisional diffusion, see figure 10 a). However, as shown in figure 10b), non-local electron currents may occur, short circuiting the radial ambipolar potential and altering the radial plasma motion. Figure 10 implies that the radial expansion is supported by non-local currents. It must be noted that the non-local currents require a conductor, such as background plasma, at large radius to carry them. Thus finite chamber size may provide the conditions for non-local currents, whereas space vacuum would not.

Such short-circuiting electron currents complicate the modeling of jet expansion. In a laboratory experiment, particularly one with nearby conducting surfaces, moderate ambient gas pressure or complex magnetic field structure, such as curvature, electrons may neutralize ion flow by several possible mechanisms and promote radial plasma flow[15]. If a background plasma (or a conducting surface) exists on the jet's path, electrons may move along (or across) magnetic lines to neutralize ion flow. If a background plasma does not exist, electrons must move across magnetic lines by collisions[15] or anomalous transport[16]. Yet another possibility is the modification of the external magnetic field lines by currents induced in plasma[17] . These scenarios realized in the laboratory are not represented in a single-fluid model. Moreover, electrons in real plasmas tend to stratify into different groups: trapped and passing; cold, warm and hot; current-conducting and ionizing[18]. These groups may have completely different transport behavior and typically can not be described by one fluid where all groups are lumped into a single "averaged" electron population. Depending on the experimental conditions, a one-fluid model may not be sufficient to describe plasma jet detachment.

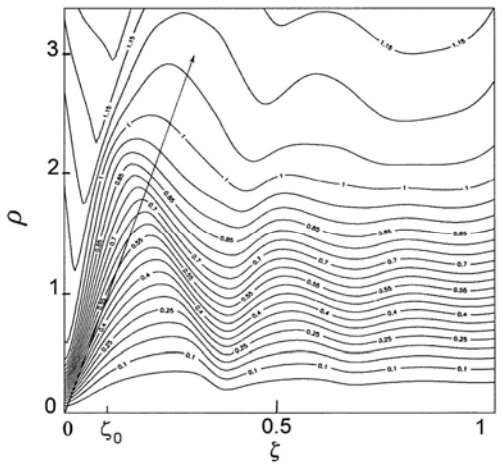

Figure 11. Ion trajectory (streamlines of ion flow) in cylindrical geometry. Ion jet propagates with a supersonic velocity along ζ and expands radially due to the electron temperature. The arrow shows the characteristic angle of plasma expansion at the sound velocity.

In summary, the non-Maxwellian ion and electron distributions found in laboratory plasmas, along with a moderate ambient neutral gas density and curved magnetic fields, mandate more complete numerical and theoretical treatments than single-fluid MHD.

V. Acknowledgments

The author thanks Y. Raitses, D. Sydorenko, S. A. Cohen, E.A. Startsev, A. Smolyakov for stimulating and helpful discussions.

VI. Conclusions

Plasmas used in electric propulsion often operate in the low-pressure regime, where particle mean free path is large compared with thruster dimensions. As a result, the collisionless effects become important and kinetic treatment has to be performed for plasma modeling. On a number of examples it is shown that the fluid approach can lead to quantitatively and qualitatively incorrect results, as the EEDF can be far from a Maxwellian. Electrons tend to stratify into different groups depending on their origin and confinement. The concept is demonstrated on an example of calculation of particle and heat losses from bounded plasma in presence of strong secondary electron emission as pertains to but not limited to a Hall thruster. Another example is plasma jet's radial expansion in presence of strong axial magnetic field, where short-circuiting flows result in a cylindrical shape of the jet in contrast to conical. A practical application of this result can be analysis of differences between testing, laboratory environment and real space environment.

VII. References

[1] Godyak, V.A., "Non-Equilibrium EEDF in Gas Discharge Plasmas", submitted to special issue of "Nonlocal electron kinetics in low pressure plasmas", IEEE Trans. on Plasma Science, 2005.

[2] Lieberman, M.A., Lichtenberg, A.J., *Principles of Plasma Discharges and Materials Processing*, 2nd ed., John Wiley & Sons Inc., New York, 2005, Chap.18.

[3] Bibinov, N.K., Bolshukhin, D.O., Wiesemann, K., "Spectroscopic determination of cold electrons in electron cyclotron resonance discharges with highly charged ions," Review of scientific instruments. Vol. 69**,** No 2, 1998, pp.1200.

[4] Zhil'tsov, V.A., Skovoroda, A.A., Timofeev, A.V., "Production of hot electrons in mirror systems associated with ECR heating with longitudinal input of microwaves", Soviet journal of plasma physics, vol. 17, No 7, 1991, pp. 447.

[5] Kaganovich, I.D., Mišina, M., Gijbels, R., and Berezhnoi, S.V., "Electron Boltzmann kinetic equation averaged over fast electron bouncing and pitch-angle scattering for fast modeling of electron cyclotron resonance discharge", Phys. Rev. E. vol. 61, 2000, pp. 1875-1889 .

[6] Berezhnoi, S.V., Kaganovich, I.D., and Tsendin, L.D., **"**Formation of cold electron population in capacitively coupled discharge as analogy of heat explosion", Plasma Physics Reports, vol.24, No 7, 1998, pp. 556-563.

[7] Polomarov, O. V., Theodosiou, C. E., Kaganovich, I. D., Economou, D. J., and Ramamurthi,B. N. "Self-consistent modeling of non-local inductively-coupled plasmas." submitted to special issue of "Nonlocal electron kinetics in low pressure plasmas", IEEE Trans. on Plasma Science, 2005.

[8] Tsendin, L.D., Sov.Phys. JETP vol. 39, 1974, pp.805.

[9] Kaganovich, I.D., Mišina, M., Gijbels, R., and Berezhnoi,S.V., "Electron Boltzmann kinetic equation averaged over fast electron bouncing and pitch-angle scattering for fast modeling of electron cyclotron resonance discharge", Phys. Rev. E. vol. 61, 2000, pp. 1875, 1889.

[10] Levistky, S.M., Journal of Technical Physics, vol.27, 157, pp. 970-1001.

[11] Sydorenko, D., Smolyakov, A., Kaganovich, I., and Raitses, Y., "Kinetic Simulation of Effects of Secondary Electron Emission on Electron Temperature in Hall Thrusters", the IEPC-05 paper 078; Sydorenko, D. Y. and Smolyakov, A. I., "Simulation of Secondary Electron Emission Effects in a Plasma Slab in Crossed Electric and Magnetic Fields," APS DPP 46th Annual Meeting, Savannah, GA, November 15-19, 2004, NM2B.008; Sydorenko, D., Smolyakov, A., Kaganovich, I., and Raitses, Y., "Modification of Electron Velocity Distribution in Bounded Plasmas by Secondary Electron Emission," Workshop "Nonlocal Collisionless Phenomena in Plasmas," Princeton Plasma Physics Laboratory, Princeton, NJ, August 2-4, 2005; to be submitted to the IEEE Transactions on Plasma Sciences.

[12] Raitses, Y., Staack, D., Smirnov, A., and Fisch N. J., "Space Charge Saturated Sheath Regime and Electron Temperature Saturation in Hall Thrusters," *Physics of Plasmas*, Vol. 12, No. 7, 2005, 073507, 10 p.

[13] Kaganovich, I., Raitses, Y., Sydorenko, D., and Smolyakov, "Effects of Non-Maxwellian EEDF on Particle and Heat Losses from a Plasma in Presence of Secondary Electron Emission," PPPL preprint, URL: http://www.pppl.gov/pub_report.

[14] Kaganovich, I. D., Shvets, G., Startsev,E., and Davidson, R. C., "Nonlinear charge and current neutralization of an ion beam pulse in a pre-formed plasma", Physics of Plasmas vol. 8, 2001, pp. 4180.

[15] Kaganovich, I.D., Rozhansky, V.A., Tsendin, L.D., Veselova, I.Yu., "Fast expansion of a plasma beam controlled by short-circuiting effects in a longitudinal magnetic field", Plasma Sources Sci. and Technol. vol.5, 1996, pp.743.

[16] Kaganovich, I.D., Rozhansky, V. A., "*Transverse conductivity in braided magnetic field*", Physics of Plasmas vol.5, 1998, pp. 3901.

[17] Arefiev, A.V. and Breizman, B.N., Institute of Fusion Science Research Report IFSR 1007, University of Texas at Austin 2004.

[18] Cohen, S. A., Siefert, N. S., Stange, S., Boivin, R. F., *et al.*, Phys. Plasmas vol.10, 2003, pp.2593.